

NATIONAL RADIO ASTRONOMY OBSERVATORY
CHARLOTTESVILLE, VA.

JUN 22 1994

Polarization Calibration of the NRAO 140-ft Telescope with Feed Rotation

M. M. McKinnon
National Radio Astronomy Observatory
Green Bank, West Virginia

May 31, 1994

Abstract

In an effort to explore the polarization properties of the NRAO 140-ft telescope, observations of the linearly-polarized radio source 3C 286 were made at different orientations of the telescope feed. The observations were made at a sky frequency of 1660 MHz with 20 MHz of bandwidth. The spectral processor was used in a polarization observing mode to measure the Stokes parameters of the source. The observations were made with both linearly and circularly-polarized feeds. The linear feed data were used to measure the linear polarization of 3C 286, giving a percent linear polarization of $m = 9.4\% \pm 0.5$ and a position angle of $\psi = 35^\circ \pm 1$.

A general model of telescope polarization, which makes no assumptions about the amplitude and phase of cross-coupling terms, and the general technique of polarization calibration are described. The model and technique are applicable to most radio telescopes. Using the known Stokes parameters of 3C 286 and the measured Stokes parameters at different feed orientations, the elements of a telescope polarization matrix are determined with a least squares fit to the model. For the circular feed data, the solution to the model indicates that the isolation between telescope IFs is about -23 dB. The cross-coupling between IFs most likely originates in the hybrid polarizer which converts linear to circular polarization. Applying the method to the linear feed data suggests that cross-coupling can be neglected when the isolation is better than -30 dB.

1 Introduction

Polarization calibration of a radio telescope requires observations of a polarization calibrator at many different orientations of the telescope's electrical axis with respect to the source. For telescopes such as the VLA and the GBT which have altitude-azimuth mounts, this coordinate transformation arises quite naturally from parallactic angle rotation. The telescope electrical axis is fixed on the sky, and the electric vector of the radio source rotates as the source passes over the telescope. However, for the equatorially-mounted 140-ft telescope, the telescope feed (receiver box) must be physically rotated to change the electrical axis with respect to the source. The response of the measured Stokes parameters of a radio source to feed rotation and parallactic angle rotation is mathematically the same; therefore, the calibration procedure proposed in this memorandum for the 140-ft telescope is applicable to other radio telescopes as well. Section 2 presents a general model of instrumental polarization, while section 3 describes the observations of 3C 286 which were used to determine the instrumental terms of the model. The percent linear polarization and position angle of 3C 286 are estimated from the uncalibrated linear feed data in section 4. The calibration procedure is applied to the circular feed data and the linear feed data in sections 5 and 6, respectively. Concluding remarks are given in section 7.

2 A Model of Instrumental Polarization

Consider an electromagnetic wave whose polarization can be described by two orthogonal components, E_x and E_y . At the radio telescope, the polarization of the wave is altered by a telescope transmission matrix, \mathbf{T} , commonly called the Jones matrix (Mott 1992).

$$\begin{bmatrix} E'_x \\ E'_y \end{bmatrix} = \begin{bmatrix} T_{xx} & T_{xy} \\ T_{yx} & T_{yy} \end{bmatrix} \begin{bmatrix} E_x \\ E_y \end{bmatrix} \quad (1)$$

The elements of \mathbf{T} are generally complex. The off-diagonal terms in the matrix are cross-coupling terms, and can originate in microwave devices such as hybrid polarizers and transfer switches. Without loss of generality, the amplitudes and phases of the matrix elements can be referenced to the amplitude, g , and phase of T_{xx} .

$$\mathbf{T} = g \begin{bmatrix} 1 & K_{xy} \exp(i\theta_{xy}) \\ K_{yx} \exp(i\theta_{yx}) & K_{yy} \exp(i\theta_{yy}) \end{bmatrix} \quad (2)$$

The phase of T_{xx} has not been included in equation 2 because it will be removed upon detection. Once the signals given by equation 1 are detected, they can be used to calculate the measured Stokes parameters of the electromagnetic wave.

$$Sm_0 = E'_x E'^*_x + E'_y E'^*_y \quad (3)$$

$$Sm_1 = E'_x E'^*_x - E'_y E'^*_y \quad (4)$$

$$Sm_2 = 2\text{Re}(E'_x E'^*_y) \quad (5)$$

$$Sm_3 = 2\text{Im}(E'_x E'^*_y) \quad (6)$$

$$(7)$$

As shown by Mott (1992), the elements of the Jones matrix can be used to construct a transmission matrix, \mathbf{M} , which relates the vector of true Stokes parameters, \mathbf{S} , to the vector of measured Stokes parameters, $\mathbf{Sm} = \mathbf{M} \cdot \mathbf{S}$. The matrix \mathbf{M} is referred to as the Mueller matrix. Since \mathbf{M} is a four-by-four matrix, it is often assumed (e.g. Thiel 1976) that a polarization calibration scheme must uniquely determine 16 instrumental terms. However, it is clear from equation 2 that only seven terms are needed to completely specify the instrumental polarization of a telescope.

The amplitudes of the cross-coupling terms in \mathbf{T} can be small, and these terms are occasionally neglected in calibration schemes. This assumption is probably well justified when linearly-polarized feeds are used, in which case the Mueller matrix is

$$\mathbf{M} = \frac{g^2}{2} \begin{bmatrix} 1 + K_{yy}^2 & 1 - K_{yy}^2 & 0 & 0 \\ 1 - K_{yy}^2 & 1 + K_{yy}^2 & 0 & 0 \\ 0 & 0 & 2K_{yy} \cos(\phi_{yy}) & 2K_{yy} \sin(\phi_{yy}) \\ 0 & 0 & -2K_{yy} \sin(\phi_{yy}) & 2K_{yy} \cos(\phi_{yy}) \end{bmatrix} \quad (8)$$

To determine the elements of \mathbf{M} , one must observe a source of known polarization at different rotation angles, β , of the telescope feed. Rotating the feed alters the Stokes parameters by a rotation matrix, $\mathbf{R}(\beta)$.

$$\hat{\mathbf{S}}(\beta) = \mathbf{M} \cdot \mathbf{R}(\beta) \cdot \mathbf{S} \quad (9)$$

The elements of $\mathbf{R}(\beta)$ depend upon polarization basis, and the appendix gives $\mathbf{R}(\beta)$ for both the linear and the circular polarization bases. Observations of a polarization calibrator at N different values of β produce a $4 \times N$

matrix of measured Stokes parameters. The elements of \mathbf{M} can be estimated by minimizing an averaged χ^2 defined by

$$\chi^2 = \frac{1}{4\sqrt{N - n_p}} \sum_{i=0}^3 \sum_{j=0}^{N-1} (Sm_{ij} - \hat{S}_{ij})^2 \quad (10)$$

where n_p is the number of fit parameters in the model. Once \mathbf{M} is known, the true Stokes parameters of a source of unknown polarization can be calculated with simple matrix inversion.

3 Observations

Observations of 3C 286 were made with the 140-foot telescope to determine the elements of \mathbf{T} . The sky frequency of the observation was 1660 MHz centered on 20 MHz of bandwidth. The spectral processor was used as a polarimeter in spectral line mode to form the detected signals. All 1024 frequency channels of the spectral processor were used in the observation. Data were recorded on and off the source at telescope feed orientations ranging from zero to 108 degrees in six degree intervals. The integration time for a single on or off-source measurement was three minutes. After subtracting the detected signal of the off-source measurement from the on-source measurement, the Stokes parameters in each frequency channel were calculated at each orientation of the telescope feed. The observations were first carried out with circularly-polarized feeds, and were repeated with linearly-polarized feeds.

4 The Linear Polarization of 3C 286

Fitting a model of instrumental polarization to the measured Stokes parameters of 3C 286 requires an accurate estimate of its true Stokes parameters. One may refer to the literature for previous measurements of the parameters, but the linear polarization of 3C 286 can be measured with the linear feed data in a manner similar to that of Mayer, McCullough, and Sloanaker (1963) or Sastry, Pauliny-Toth, and Kellerman (1967). Both experiments employed the feed rotation technique, and, in each case, the linear polarization was estimated by fitting the experimental data to a sinusoid which varied with rotation angle. In the case of $K_{yy} \approx 1.0$ and $S_1/S_0 \ll 1.0$, it

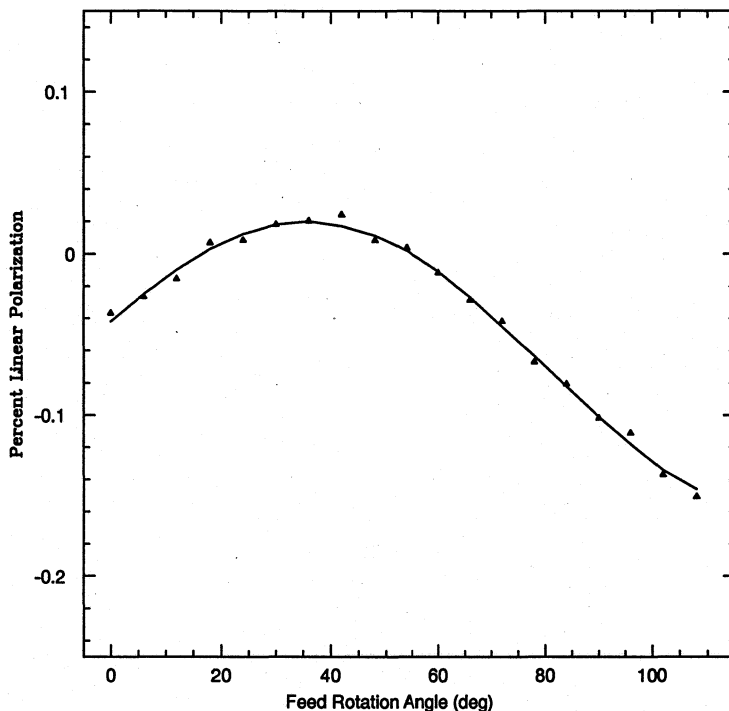


Figure 1: The percent linear polarization of 3C 286 as a function of feed rotation angle. Triangles are the data from channel 400 of the spectral processor, and the solid line is the model fit.

can be shown from equations 8 and 9 that the quantity $y = Sm_1/Sm_0$ will vary with rotation angle, β , as

$$y(\beta) \simeq b + m \cos[2(\beta - \psi)] \quad (11)$$

where the amplitude, m , of the sinusoid is the percent linear polarization of 3C 286, the phase, ψ , is its intrinsic position angle, and the bias offset is $b \simeq (1 - K_{yy}^2)/(1 + K_{yy}^2)$. Note that y takes on its maximum value when $\beta = \psi$ where one of the linear feeds is aligned with the electric vector of 3C 286. A standard least squares fit to equation 11 was made with the data from each frequency channel of the spectral processor using the grid search method (Bevington and Robinson, 1992). Uniform weighting was used in the fit. The initial estimates of b , m , and ψ for the fit to the data of a channel were made with the solution to the data from the previous frequency channel.

An example fit to the data in channel 400 is shown in Figure 1. The fit parameters for channel numbers 50 through 975 are summarized in Figure 2. The channels at the edges of the observing band were not used because tests indicate that the Stokes parameters are not accurately reproduced in those parts of the band (McKinnon 1994). As shown in Figure 2a, the χ^2 of the fit for most channels is roughly the same, indicating that equation 11 represents the data in each channel equally well. Figure 2c shows no indication of Faraday rotation as one might expect for 3C 286 at the sky frequency of the observation. The percent polarization and position angle averaged over the band are $m = 9.35\% \pm 0.16$ and $\psi = 34.6^\circ \pm 0.6$, respectively, in good agreement with the results of Morris and Berge (1964, see Table 1). The entries in Table 1 for this work reflect estimates of the systematic errors of the experiment. Knowing m and ψ , one may construct the vector of true Stokes parameters of 3C 286. If 3C 286 has no circular polarization, the vector is

$$\mathbf{S} = I \begin{bmatrix} 1 \\ m \cos(2\psi) \\ m \sin(2\psi) \\ 0 \end{bmatrix} \quad (12)$$

where I is the flux density of 3C 286 at the observing frequency. The vector used in the calibration procedures which follow was calculated from equation 12 using the quantities in the last column of Table 1.

Reference Wavelength (cm)	MB 1964 21.2	MB 1964 18.0	This Work 18.1
$m(\%)$	9.3 ± 0.5	8.7 ± 0.7	9.4 ± 0.5
ψ (deg)	32 ± 2	34 ± 5	35 ± 1

Table 1: The percent linear polarization, m , and the position angle, ψ , of 3C 286 compared to the measurement of Morris and Berge (1964).

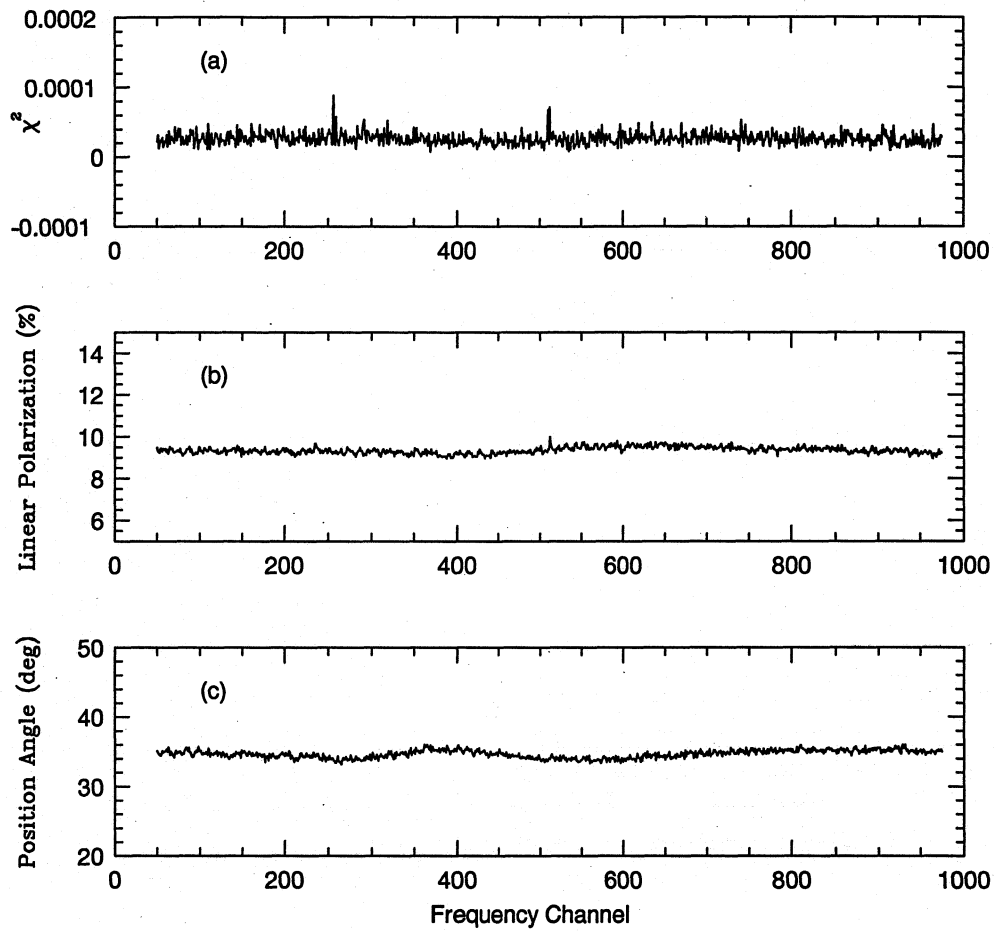


Figure 2: The percent linear polarization (b) and the position angle (c) of 3C 286 in each frequency channel of the spectral processor as determined from a least squares fit. The goodness of the fit (a) is relatively constant across the band.

5 Calibration in the Circular Polarization Basis

The data collected with circularly-polarized feeds were used to estimate the Mueller matrix for each frequency channel of the spectral processor by minimizing the χ^2 given in equation 10. The solution to the data from channel 526 is shown in Figure 3. The Mueller matrix found for channel 526 is listed in Table 2. Figure 4 shows the χ^2 , K_{yy} , and θ_{yy} determined from the fit to the data from channels 50 through 975. Again, the χ^2 is relatively constant across the band, suggesting that the model describes the data in each channel equally well. Figure 5a shows the amplitudes of the cross-coupling terms expressed in decibels of isolation ($dB = 20 \log_{10}(K)$). The phases of the cross-coupling terms are displayed in Figure 5b. The apparent lack of noise in K_{yx} and θ_{yx} is most likely due to limitations of the grid search used to minimize χ^2 . The average isolation across the band is no better than -23 dB, consistent with the isolation (-25 dB) predicted by the manufacturer of the hybrid polarizer. The polarizer is used to convert linear to circular polarization.

	M_{i0}	M_{i1}	M_{i2}	M_{i3}
M_{0j}	0.94	0.07	-0.04	-0.07
M_{1j}	0.07	0.93	-0.06	0.06
M_{2j}	0.09	0.01	-0.61	-0.71
M_{3j}	0.02	0.08	0.70	-0.60

Table 2: The Mueller matrix for frequency channel 526.

Convergence of the grid search algorithm was tested by varying the initial estimates of the instrumental terms. This test indicated that the quantities g , K_{yy} , and θ_{yy} are determined to an accuracy of three significant figures, but the cross-coupling terms are only accurate to about 3 dB of isolation and about 20° of phase.

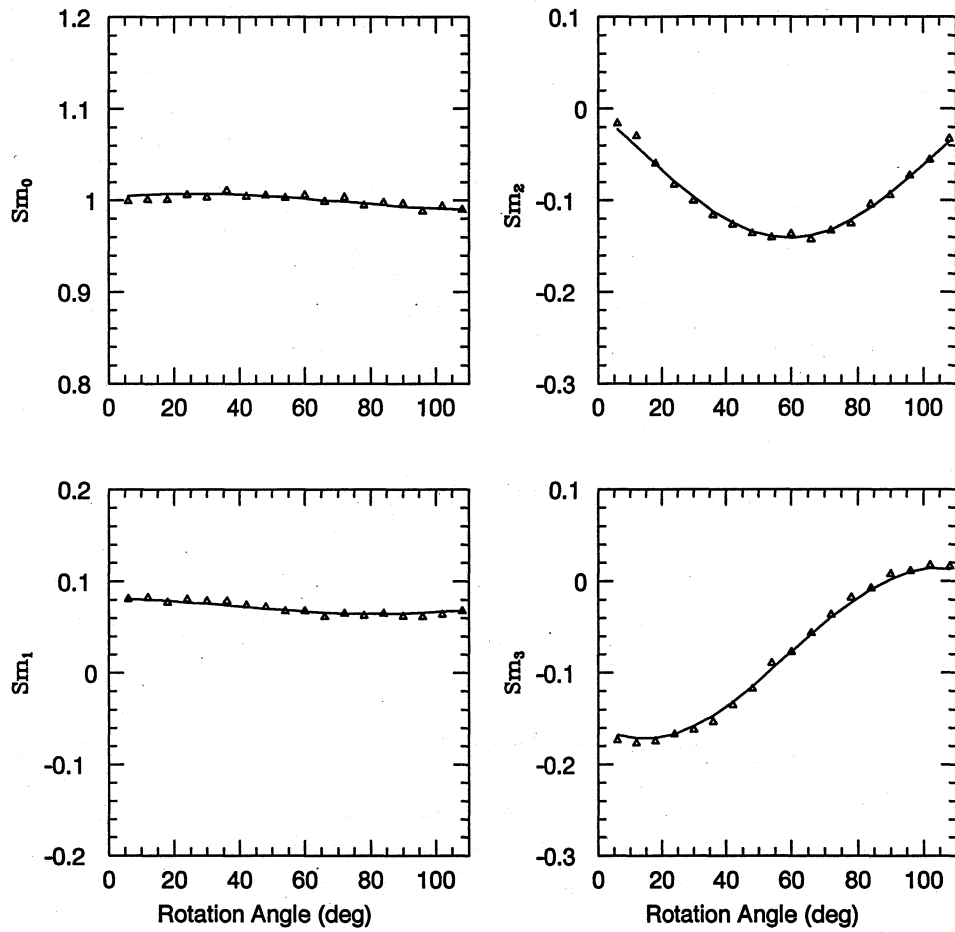


Figure 3: The measured Stokes parameters of 3C 286 (triangles) in channel 526 of the spectral processor. The solid lines represent the model fit to the data.

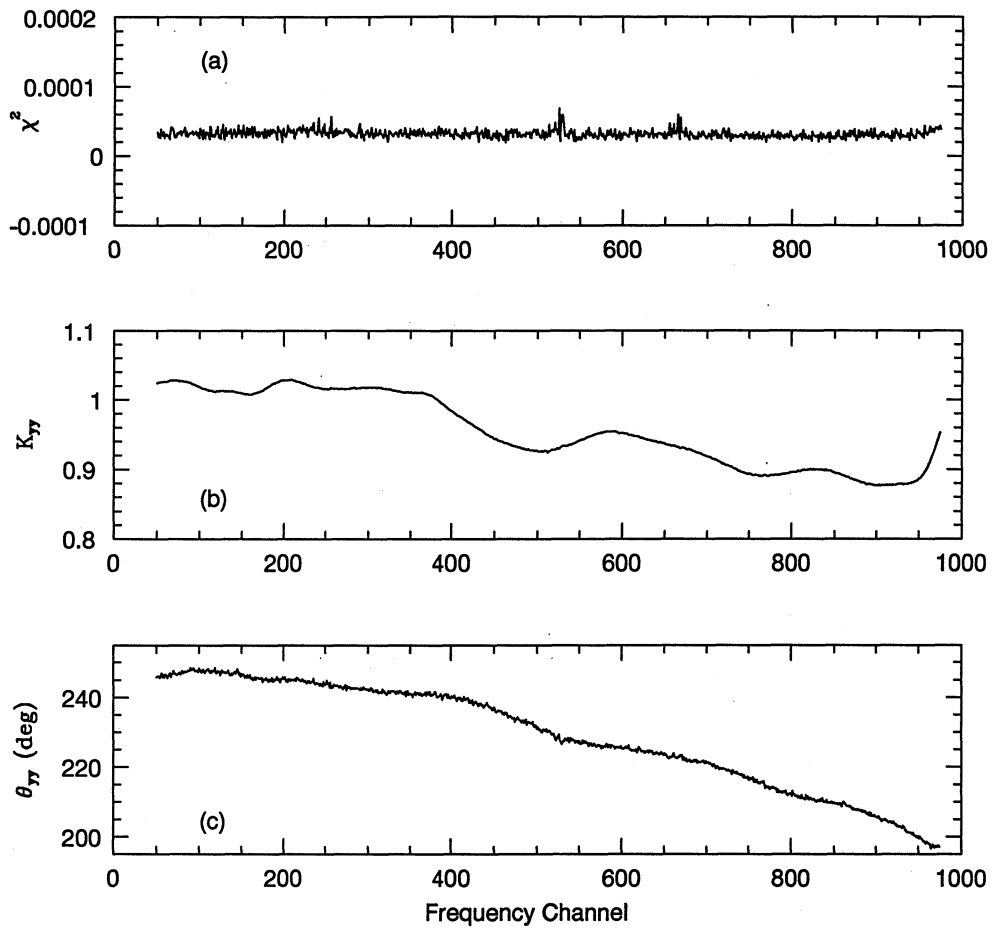


Figure 4: The χ^2 (a), IF gain imbalance (b), and IF phase difference (c) determined from a fit to the circular-feed data in each channel of the spectral processor.

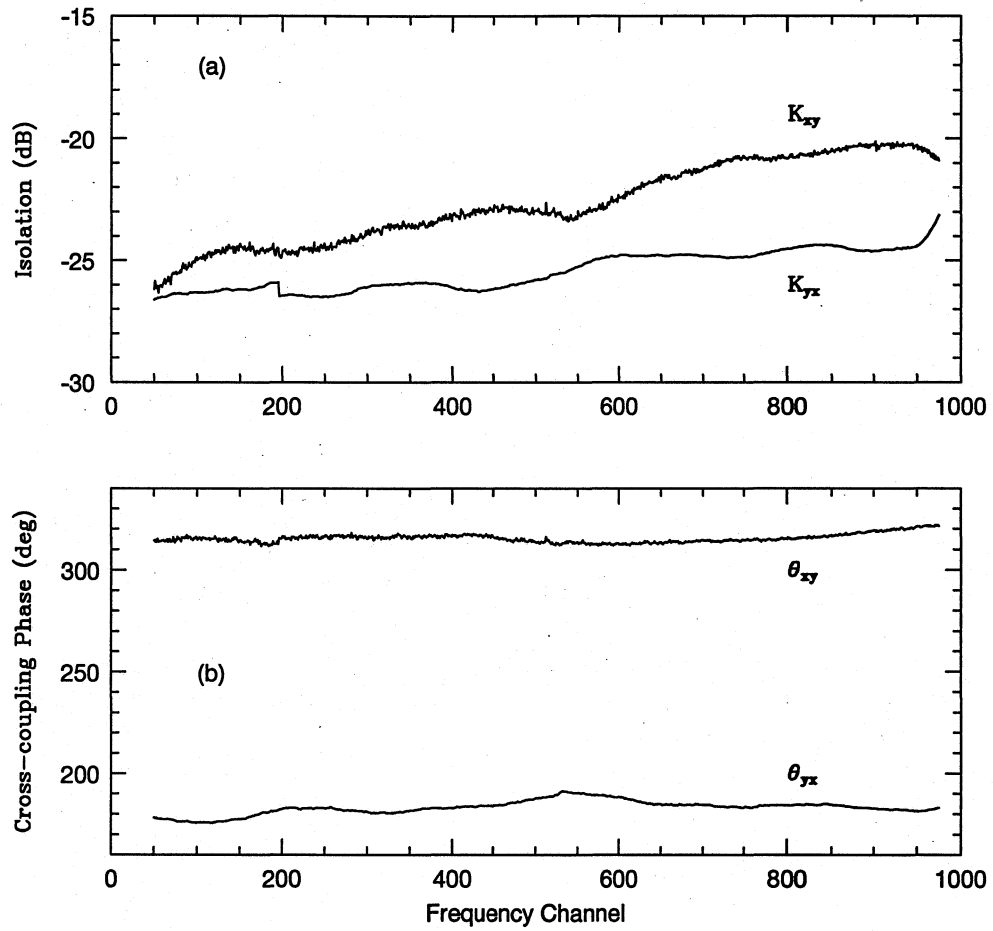


Figure 5: The isolation (a) and phase (b) of the IF cross-coupling terms determined from a fit to the circular-feed data in each channel of the spectral processor.

Errors in the elements of M can arise from inaccurate estimates of the Stokes parameters of 3C 286. To test this potential source of error, the analysis was repeated using the polarization tabulated by Perley (1982; $m = 0.098$, $\psi = 33^\circ$). The solution showed no significant deviations from the original results.

6 Calibration in the Linear Polarization Basis

The seven-parameter fit to the linear feed data produced cross-coupling terms with very small amplitudes. The isolation ranged from -28 to -35 dB. However, the cross-coupling terms were highly covariant, and thus poorly determined. A three-parameter fit to the Mueller matrix given by equation 8 produced χ^2 values which were consistent with those obtained with the seven-parameter fit, suggesting that cross-coupling can be neglected at the -30 dB level. The solution to the three-parameter fit is shown in Figure 6. Although there are variations in χ^2 across the band, they are not significant; therefore, the model probably describes the data in most frequency channels equally well.

The measurement of the linear polarization of 3C 286 in section 4 was based upon two assumptions: $K_{yy} \approx 1.0$ and $m \ll 1.0$. These assumptions can probably be justified since it was found that $m = 0.094$, consistent with previous work, and Figure 6 shows that the gain ratio is in the range $0.92 < K_{yy} < 1.14$. The analysis in section 4 also predicted a relationship between K_{yy} and the bias offset, b , of the sinusoid fit. To check the sinusoid fit and the three-parameter fit for consistency, a residual defined by

$$R = \frac{1 - K_{yy}^2}{1 + K_{yy}^2} - b \quad (13)$$

was calculated for each frequency channel (Figure 7). Although there are some low-level systematic offsets in R , the average value of $R = 8.4 \times 10^{-4} \pm 1.0 \times 10^{-3}$ suggests that the two fit procedures are consistent.

7 Discussion and Conclusions

Polarimetry with the NRAO spectral processor holds much promise because calibration on a channel-by-channel basis reduces the measurement error which might otherwise be incurred with a broad-band polarimeter. As one

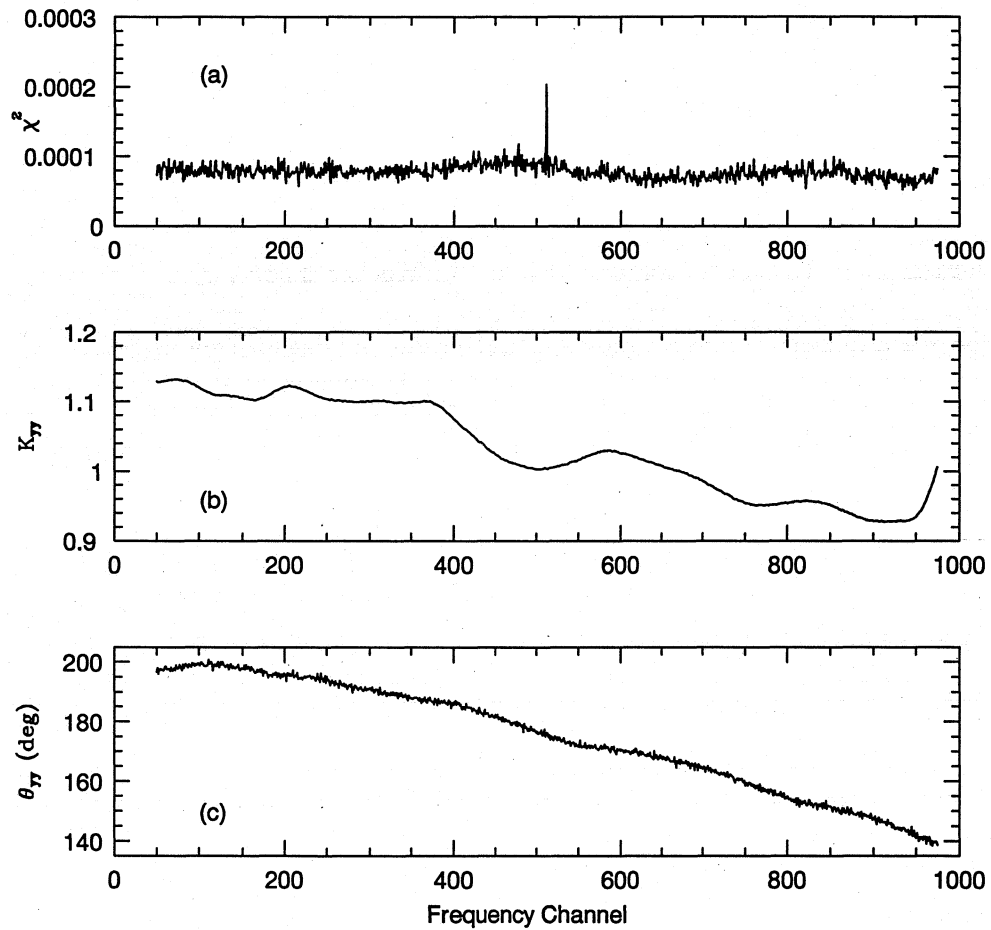


Figure 6: The χ^2 (a), IF gain imbalance (b), and IF phase difference (c) determined from a three-parameter fit to the linear-feed data in each channel of the spectral processor.

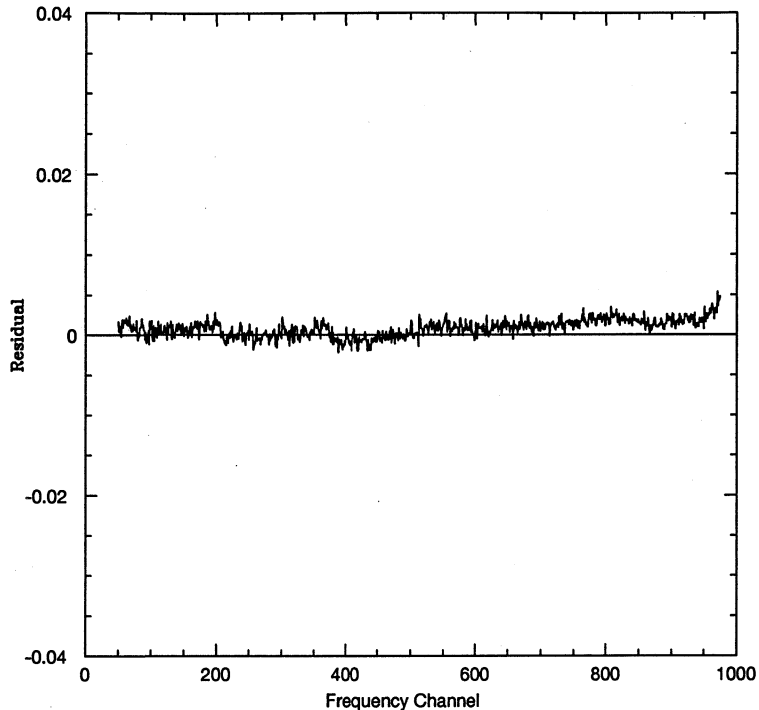


Figure 7: A test for consistency between the three-parameter fit and the percent polarization fit. A zero residual (see the text for its definition) implies consistency.

could imagine from Figures 4 and 6, the errors can be significant if the measured Stokes parameters are averaged over a broad observing band.

Comparisons of Figure 4b with Figure 6b and Figure 4c with Figure 6c show that the variations in the instrumental terms across the band are remarkably similar for the circular and linear feed data. Since linear polarization is converted to circular polarization in the RF section of the telescope, these comparisons suggest that the spectral variations of the instrumental terms occur primarily in the IF section of the telescope. Had the variations occurred in the RF section, one might suspect that the circular polarization was improperly generated.

While investigating the polarization properties of the Arecibo telescope, Stinebring et al. (1984) found that the cross-coupling terms in \mathbf{T} are orthogonal ($K_{xy} = K_{yx}$ and $\theta_{xy} = \theta_{yx} \pm \pi$). This property simplifies the problem of calibration since five, instead of seven, instrumental terms must

be determined. As Stinebring et al. show, the mathematics of the problem become even simpler when the amplitudes of the cross-coupling terms are small ($K_{xy}, K_{yx} \ll 1.0$). Figure 5 indicates that the cross-coupling terms of the 140-foot telescope are not orthogonal. However, the amplitudes of the cross-coupling terms are small, so the mathematics can be simplified (thus reducing the number of computer operations in the calibration procedure) by neglecting terms of order K_{xy}^2 and K_{yx}^2 .

The primary objective of this memorandum has been to illustrate the technique of polarization calibration with feed or parallactic angle rotation. Future applications of the technique can be improved with a more robust algorithm to minimize χ^2 . Optimization of observing procedures for quick calibration may allow for an investigation of the temporal stability of the instrumental polarization.

I thank J. R. Fisher and B. Vance for assistance with the observations.

References

- [1] Bevington, P. R. and Robinson, D. K., 1992, *Data Reduction and Error Analysis for the Physical Sciences*, (New York, McGraw-Hill)
- [2] Mayer, C. H., McCullough, T. P., and Sloanaker, R. M., 1963, *ApJ* 139, 248
- [3] McKinnon, M. M. 1992, *A & A* 260, 533
- [4] McKinnon, M. M. 1994, *A Test of a Polarization Observing Mode on the NRAO Spectral Processor*, NRAO Spectral Processor Memo. 35
- [5] Morris, D. and Berge, G. L., 1964, *AJ* 69, 641
- [6] Mott, H., 1992, *Antennas for Radar and Communications: A Polarimetric Approach*, New York: Wiley
- [7] Perley, R. A., 1982, *AJ* 87, 859
- [8] Sastry, Ch. V., Pauliny-Toth, I. I. K., and Kellerman, K. I., 1967, *AJ* 72, 230
- [9] Stinebring, D. R., Cordes, J. M., Rankin, J. M., Weisberg, J. M., and Boriakoff, V., 1984, *ApJS* 55, 247

[10] Thiel, M. A. F., 1976, J. Opt. Soc. Am. 66, 65

A Rotation Matrices

For a counterclockwise rotation of the telescope feed by an angle β in the frame of the observer, the rotation matrix in the circular polarization basis is

$$\mathbf{R}(\beta) = \begin{bmatrix} 1 & 0 & 0 & 0 \\ 0 & 0 & 0 & 1 \\ 0 & \cos(2\beta) & \sin(2\beta) & 0 \\ 0 & -\sin(2\beta) & \cos(2\beta) & 0 \end{bmatrix} \quad (14)$$

In the linear polarization basis, the rotation matrix is

$$\mathbf{R}(\beta) = \begin{bmatrix} 1 & 0 & 0 & 0 \\ 0 & \cos(2\beta) & \sin(2\beta) & 0 \\ 0 & -\sin(2\beta) & \cos(2\beta) & 0 \\ 0 & 0 & 0 & 1 \end{bmatrix} \quad (15)$$